Chemical Engineering Journal 154 (2009) 287–294

Contents lists available at ScienceDirect

Chemical Engineering Journal

journal homepage: www.elsevier.com/locate/cej

Production of hydrogen from thermo-catalytic decomposition of methane in a fluidized bed reactor

P. Ammendola[a,*], R. Chirone[a], G. Ruoppolo[a], G. Russo[b]

[a] Istituto di Ricerche sulla Combustione, CNR, P.le V. Tecchio, 80, 80125 Napoli, Italy
[b] Dipartimento di Ingegneria Chimica, Università degli Studi di Napoli Federico II, P.le Tecchio, 80, 80125 Napoli, Italy

ARTICLE INFO

Keywords:
Hydrogen production
Methane decomposition
Fluidized bed
Methane concentration
Temperature
Contact time
Controlling regime

ABSTRACT

The Thermo-Catalytic Decomposition (TCD) of methane has been investigated in a laboratory scale bubbling fluidized bed reactor using a copper dispersed on γ-alumina as a catalyst. The effects of both total flow rate and amount of catalyst, i.e. contact time, as well as of reaction temperature and CH_4 inlet concentration on CH_4 to H_2 conversion, amount of carbon deposited on the catalyst and deactivation time have been investigated. The relevance of attrition phenomena have been also investigated as a useful way to mechanically regenerate the catalyst, removing the carbon deposited on the external surface of catalytic particles.

Samples of bed catalytic particles after TCD tests have been characterized by means of different techniques: (i) elemental analysis to obtain the amount of carbon deposited on the catalyst; (ii) SEM/EDS analysis to determine the morphology of carbon deposited on the catalyst surface; (iii) BET analysis to obtain the surface areas of deactivated catalyst.

Different dimensionless groups have been compared in order to quantitatively assess the relative importance of intrinsic kinetics and of intraparticle and interphase (bubbles to emulsion phase and emulsion phase to catalyst particle) diffusional resistances and to highlight the controlling regimes under the various operating conditions.

1. Introduction

The Thermo-Catalytic Decomposition (TCD) of CH_4 is an attractive process for the production of H_2 with reduced CO_2 emissions [1,2]. Main advantages of the TCD process compared to the CH_4 steam reforming are [1]: (i) the energy requirement is less (37.8 kJ/molH_2) than steam reforming (63.0 kJ/molH_2); (ii) the amount of CO_2 emissions is less (0.05 molCO_2/molH_2) than steam reforming (0.05 molCO_2/molH_2); (iii) it is possible to produce pure H_2; (iv) the process is very simple (no water gas shift, CO_2 separation and CO-PROX units). Nevertheless, a catalyst would be necessary since the thermal decomposition of methane would require high temperatures (above 1200 °C) [1,2], even if it deactivates due to produced carbon deposition on its surface.

Fluidized bed reactors have been recently indicated [3–8] as an efficient reactor solution for TCD process to overcome the limits linked to the use of fixed bed reactors, proposed in the past [1]: (i) relatively high pressure drops, increased by the accumulation of carbon in the bed; (ii) impossibility of a continuous operation due to the necessity to unload carbon and in turn to regenerate the catalyst; (iii) no good temperature control in both the methane decomposition and the catalyst regeneration phase. Moreover, it is to consider a possible positive effect of attrition phenomena active in fluidized beds in removing the deposited carbon from the catalyst surface.

However, new criteria have to be taken into account for catalyst design. In particular, a suitable catalyst should be characterized by a low propensity to attrition in addition to the requirements of high thermal stability and activity [9].

Catalytic systems containing Ni [10,11] and Fe [12,13] have been largely tested. The Ni based catalysts have a maximum operative temperature of about 600 °C. Being methane conversion thermodynamically limited at this temperature, concentrated hydrogen streams (H_2 > 60%) cannot be obtained using nickel based catalysts [9]. On the contrary, Fe based catalysts are more stable at higher temperatures (700–1000 °C), but deactivation occurs upon repeated cycles, resulting in a short lifetime [9]. The deposited carbon has generally a filamentous form (nanofibres or nanotubes) with metal particles on their tips.

Muradov et al. [1,2] have investigated the feasibility of using activated carbon and carbon black as catalysts. The use of carbon catalysts is advantageous on the basis of a low cost, a high temperature resistance and a large tolerance to potentially harmful compounds, even if the carbon catalysts have a lower catalytic

* Corresponding author. Tel.: +39 081 7682233; fax: +39 081 5936936.
E-mail address: paola.ammendola@irc.cnr.it (P. Ammendola).

1385-8947/$ – see front matter © 2009 Elsevier B.V. All rights reserved.
doi:10.1016/j.cej.2009.03.048

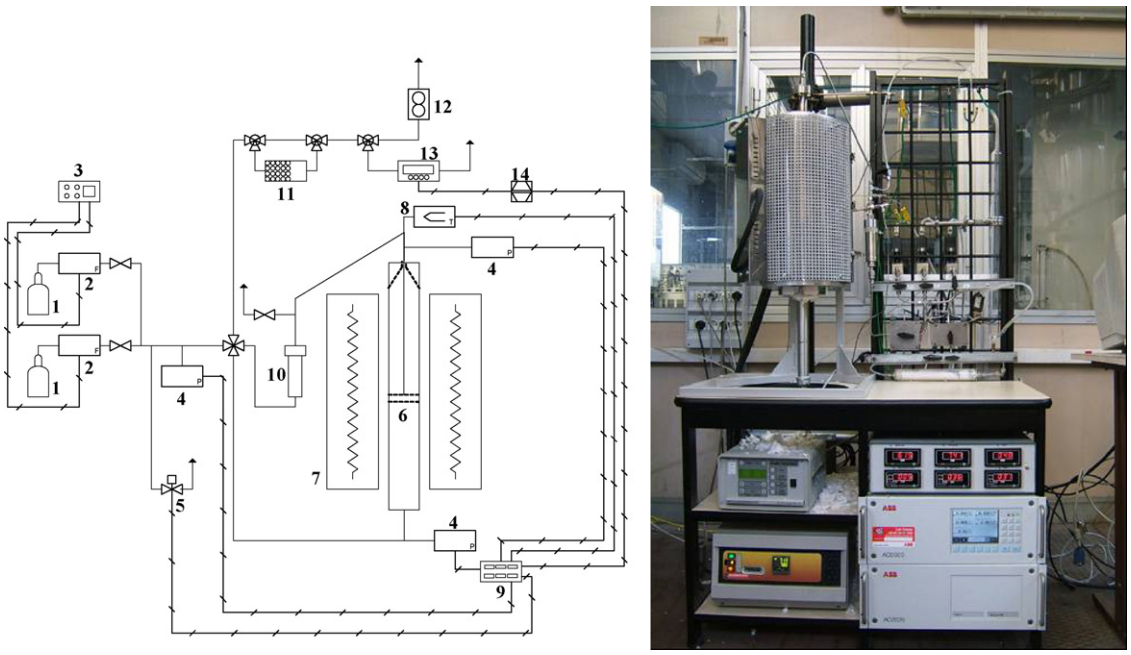

Fig. 1. Experimental apparatus: (1) cylinder; (2) flow meter; (3) controller; (4) pressure transducer; (5) solenoid valve; (6) fluidized bed reactor; (7) oven; (8) thermocouple; (9) display; (10) ceramic filter; (11) water trap; (12) flow meter; (13) analyzers; (14) PC.

activity with respect to metal catalysts and require a periodical unload/re-activation because the produced carbon is less active than the initial carbon catalyst.

Ammendola et al. [14] have proposed a suitable copper dispersed on γ-alumina catalyst. Characteristics of this catalytic system are: (i) relatively high activity (between that of carbon and Ni catalysts); (ii) high operative temperature (up to 1000 °C); (iii) relatively high mechanical resistance to attrition; (iv) carbon deposition without formation of fibres with metal particles on their tips.

In the present paper, the TCD of methane has been investigated in a laboratory scale bubbling fluidized bed reactor using the above-described copper dispersed on γ-alumina as a catalyst. The effects of both total flow rate and amount of catalyst, i.e. contact time, as well as of reaction temperature and CH_4 inlet concentration on CH_4 to H_2 conversion, amount of carbon deposited on the catalyst and deactivation time have been investigated. The relevance of attrition phenomena have been also investigated as a useful way to mechanically regenerate the catalyst, removing the carbon deposited on the external surface of catalytic particles.

Samples of bed catalytic particles after TCD tests have been characterized to obtain the amount and the morphology of carbon deposited on the catalyst surface as well as the surface areas of deactivated catalyst.

Different dimensionless groups have been compared under the various operating conditions in order to quantitatively assess the role of the different processes at work and of the controlling conversion regimes.

2. Experimental

The fluidized bed apparatus used is reported in Fig. 1. It consists of a 2.6 cm ID reactor made of alumina, equipped with a ceramic foam gas distributor, an electrical oven surrounding the reactor employed to heat up the reactor to the reaction temperature and to provide enough heat for methane decomposition, a device for collecting fine particles larger than 300 nm escaping from the reactor in the exit gases. Temperature and pressure drops have been measured by means of thermocouples vertically inserted in the reactor and pressure transducers, respectively. The inlet and outlet streams were analyzed by an on line continuous analyzer for CO, CO_2, CH_4, (ABB URAS 14) H_2 (ABB CALDOS 17) and O_2 (ABB MAGNOS 106). Methane (99.995 vol.%) and nitrogen (99.9999 vol.%) have been used without further purification.

A copper based catalyst, prepared by wet impregnation dissolving the required amount of copper acetate in aqueous solution and adding a suitable amount of high mechanical resistance γ-Al_2O_3 (Sasol) has been used. Details of the catalyst formulation are reported elsewhere [14]. Table 1 reports the main characteristic of the catalyst. The copper phase has been identified as a surface $CuAl_2O_4$. The catalytic particles used (300–400 μm) belong

Table 1
Catalyst properties.

Active phase	Copper content (wt%)	Surface area (m^2/g)	Particle size (μm)	Particle density (kg/m^3)	Geldart's classification [13]
Surface spinel $CuAl_2O_4$	8.4	156	300–400	1900	B group

Table 2
Operating conditions.

	Methane concentration (vol.%)	Reaction temperature (°C)	Total flow rate (N l/h)	Catalyst amount (g)
Effect of methane concentration	5–50	800	45	25
Effect of reaction temperature	5	700–850	45	25
Effect of total flow rate	5	800	30–60	25
Effect of catalyst amount	5	800	45	9–45

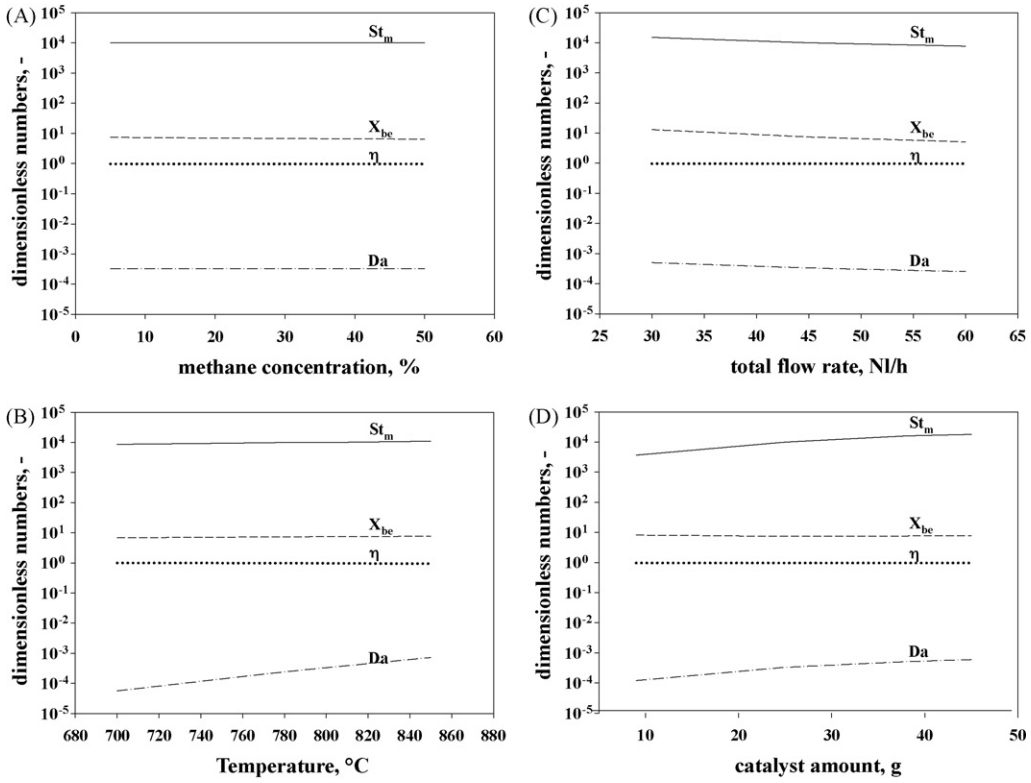

Fig. 2. Dimensionless groups as functions of methane concentration (A), reaction temperature (B), total flow rate (C) and catalyst amount (D).

to group B of Geldart's classification of powders [15]. Mechanical resistance of the catalyst has been tested by operating a bed of the catalyst at 800 °C under conditions of purely mechanical attrition for 15 h at a superficial gas velocity of 11.6 cm/s. A relatively low average attrition rate (1.5×10^{-5} g/min) has been obtained.

Methane decomposition tests have been carried out in order to investigate the effect of different operating conditions as reported in Table 2: (i) methane concentration (5–50 vol.% in N_2 flow); (ii) reaction temperature (700–850 °C); (iii) total flow rate (30–60 N l/h); (iv) catalyst amount (9–45 g). Under the different operating conditions there were practically no thermodynamic limitations to methane conversion, being the methane equilibrium conversion in the range 94–99%.

The experimental values of the minimum fluidization velocity (u_{mf}) at different bed temperatures in the range 700–850 °C, obtained by working out the pressure drop curves versus the superficial gas velocity, are in good agreement with those expected on the basis of Wen and Yu literature correlation [16], ranging from 3.1 to 2.8 cm/s, respectively. In all cases, the fluidized bed reactor has been operated under a bubbling fluidization regime.

The absence of catalytic effects due to the alumina components of the reactor or due to the catalyst support have been verified by means of preliminary tests carried out operating the apparatus with an inert bed made of quartz or alumina particles used as catalytic support, respectively.

During each test the time-resolved profiles of pressure drops, bed temperature and concentrations of different species analyzed have been recorded. A carbon balance gave the amount of produced carbon.

Samples of bed catalytic particles after TCD tests have been characterized by means of different techniques. The elemental analysis to obtain the amount of carbon deposited on the catalyst has been performed by the analyzer CHN2000 LECO. The SEM/EDS analysis, carried out using a scanning electron microscopy (Philips XL30), has been used to determine the morphology of carbon deposited on the catalyst surface. BET measurements have been also performed on deactivated catalysts with a Quantachrome Autosorb 1-C analyzer to obtain their surface areas.

The amount of carbon in the exit gas has been measured by collecting the elutriated material during the different methane decomposition tests and analyzing its carbon content.

3. Results and discussion

Preliminarily, numerical computations have been carried out in order to quantitatively assess the relative importance of intrinsic kinetics and of intraparticle and interphase (bubbles to emulsion phase and emulsion phase to catalyst particle) diffusional resistances and to highlight the controlling regimes under the various operating conditions. To this end the values of different dimensionless groups have been compared under the various operating conditions. In particular, Fig. 2 compares the values of the mass transfer Stanton number St_m, of the bubble to emulsion phase mass transfer index X_{be}, of the catalyst effectiveness factor η and of the Damkölher number Da, computed at different methane concentrations (A), reaction temperatures (B), total flow rates (C) and catalyst amounts (D), respectively. It is useful recalling that Da, St_m and X_{be} express the ratio between the gas space–time and the time of heterogeneous reaction, diffusion across the particle boundary layer and the mass transfer between the bubbles and the emulsion phase, respectively. Parameters used for the computations of different dimensionless groups are reported elsewhere [17]. Analysis of Fig. 2 indicates that St_m is orders of magnitude greater than the other numbers throughout the respective operating condition range. This finding indicates that mass transfer in the boundary layer around the catalyst particle is extremely efficient when compared with other physico-chemical processes occurring in the reactor. The catalyst effectiveness factor η is always unitary, indicating that no internal diffusion limitations occur in all cases. Moreover, X_{be} is much greater than Da, i.e. mass trans-

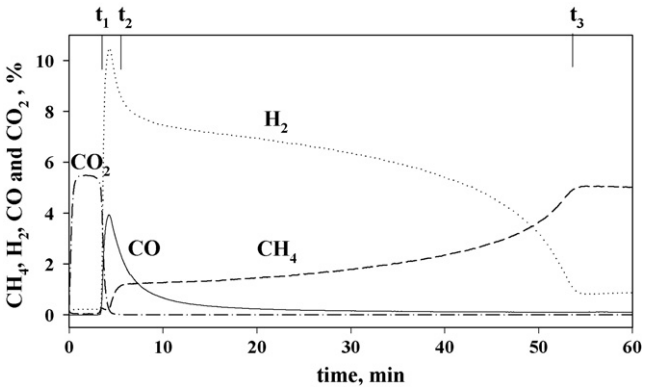

Fig. 3. SEM images of deactivated catalytic samples. (A) Feed composition: CH_4 (20 vol.%) in N_2; $T = 800\,^{\circ}C$; $m_{cat} = 25$ g; $Q = 45$ N l/h. (B) Feed composition: CH_4 (5 vol.%) in N_2; $T = 700\,^{\circ}C$; $m_{cat} = 25$ g; $Q = 45$ N l/h.

fer between bubbles and emulsion phase is more effective than intrinsic kinetics. In conclusion, in all the investigated operating conditions the methane conversion rate is controlled by the intrinsic kinetics.

Typical curves of CH_4 conversion and of H_2 production obtained during a TCD test carried out in the bubbling fluidized bed reactor are reported in Fig. 3. At time $t = 0$ an inlet gas made of CH_4 (5 vol.%) and N_2 is fed to the reactor. Analysis of the curves shows that there are three stages. Firstly ($t < t_1$), all the methane reacts with the oxygen (linked to the copper) of the oxidized catalyst according to the total oxidation reaction ($4O_s + CH_4 \rightarrow CO_2 + 2H_2O$). This reaction is faster than those of decomposition and partial oxidation. After this initial step ($t_1 < t < t_2$), CH_4 still reacts with the residual oxygen O_s of the catalyst according to CH_4 partial oxidation reaction ($O_s + CH_4 \rightarrow CO + 2H_2$), probably due to the reduced O_s availability, and CO and not CO_2 is produced. Accordingly, CO monotonically decreases corresponding to the consumption of the O_s present in the catalyst. At the same time the decomposition reaction ($CH_4 \rightarrow 2H_2 + C$) also occurs and H_2 is produced according to both methane partial oxidation and decomposition reactions, justifying the initial hydrogen peak. At times $t_2 < t < t_3$ CH_4 is mainly decomposed according to the decomposition reaction while the partial oxidation reaction is quite suppressed because O_s availability is poor; as a consequence rather limited CO concentration is measured. As time increases decomposition rate decreases as a result of the decrease of catalyst activity due to carbon deposition. However, CH_4 conversion does not drop to zero and a relatively low residual conversion is observed, probably related to a catalytic activity played by the deposited carbon [18]. A reduction pre-treatment by H_2 at $800\,^{\circ}C$ suppresses the CO_2 formation and reduces the amount of CO produced. Accordingly, the catalyst deactivation time is defined as $t_3 - t_1$.

Similar concentration profiles have been obtained under the different operating conditions investigated.

The data that will be shown in the next part of the paper refer to the third and fourth stages, when only methane decomposition occurs.

Samples of deactivated catalysts after the different methane decomposition tests have been characterized by means of different techniques in order to evaluate the occurrence of pore blocking causing the catalyst deactivation and to detect the deposited carbon morphology.

The BET analysis showed that deactivated samples, even those with higher amounts of deposited carbon, still have high surface areas (120–156 m^2/g), indicating that no pore occlusion occurs.

SEM analysis carried out on the samples after methane decomposition tests (Fig. 4), even on those with higher amounts of deposited carbon, showed that no carbon fibres with the metal particles on their tips grew on the catalyst surface up to $800\,^{\circ}C$, in contrast with that observed for nickel and iron based catalysts. The carbon produced during the decomposition is uniformly dispersed on the surface of the catalyst.

The amount of carbon deposited on the samples after methane decomposition tests, determined by carbon elemental analysis of samples, is in agreement with the stochiometric amount calculated by the carbon balance on species consumed and produced during the CH_4 decomposition tests. This analysis also shows that the deposited carbon is very poorly hydrogenate (H/C ratio is very close to zero).

Results showing the effect of methane concentration in the feed are reported in Fig. 5 in terms of methane conversion (A), amount of deposited carbon (B), carbon formation rate (C), deactivation time (D), total amount of carbon deposited on the catalyst (E) and carbon elutriation rate (F). It may be observed that higher methane concentrations lead to lower conversions and shorter deactivation times. It is to note that the observed conversions are much lower than those respectively achievable at the equilibrium. A possible explanation of the decrease of methane conversion with methane concentration is linked to intrinsic kinetics of the heterogeneous methane decomposition reaction. In particular, assuming a perfectly mixed flow (CSTR) for the emulsion phase [17], the initial values of methane conversion have been worked out obtaining a kinetic reaction order of 0.7 with respect to methane concentration. The general shapes of the curves of deposited carbon amount versus time (Fig. 5B) show a progressive increase in the deposited carbon with the reaction time up to a maximum value, at which the catalyst becomes deactivated. The carbon formation rate curves (Fig. 5C) have been obtained from the numerical derivative of the respective experimental deposited carbon amount versus time curves (Fig. 5B). All the carbon forma-

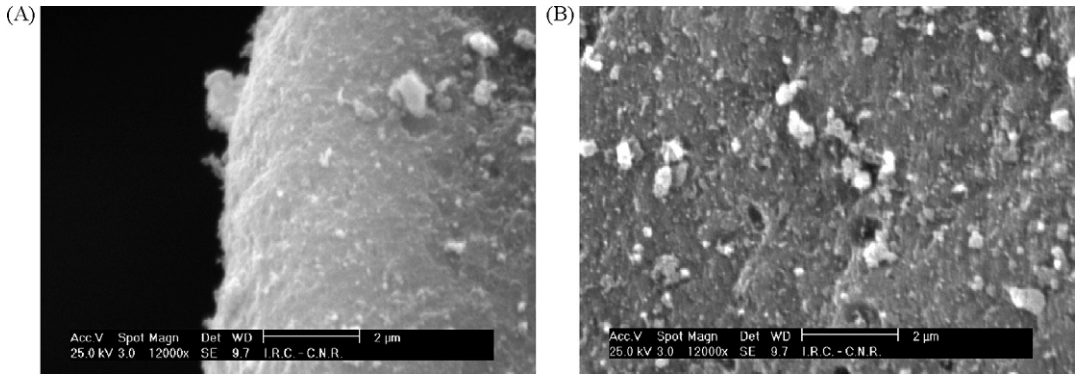

Fig. 4. Typical methane decomposition test in the fluidized bed reactor. Feed composition: CH_4 (5 vol.%) in N_2; $T = 800\,^{\circ}C$; $m_{cat} = 25$ g; $Q = 45$ N l/h.

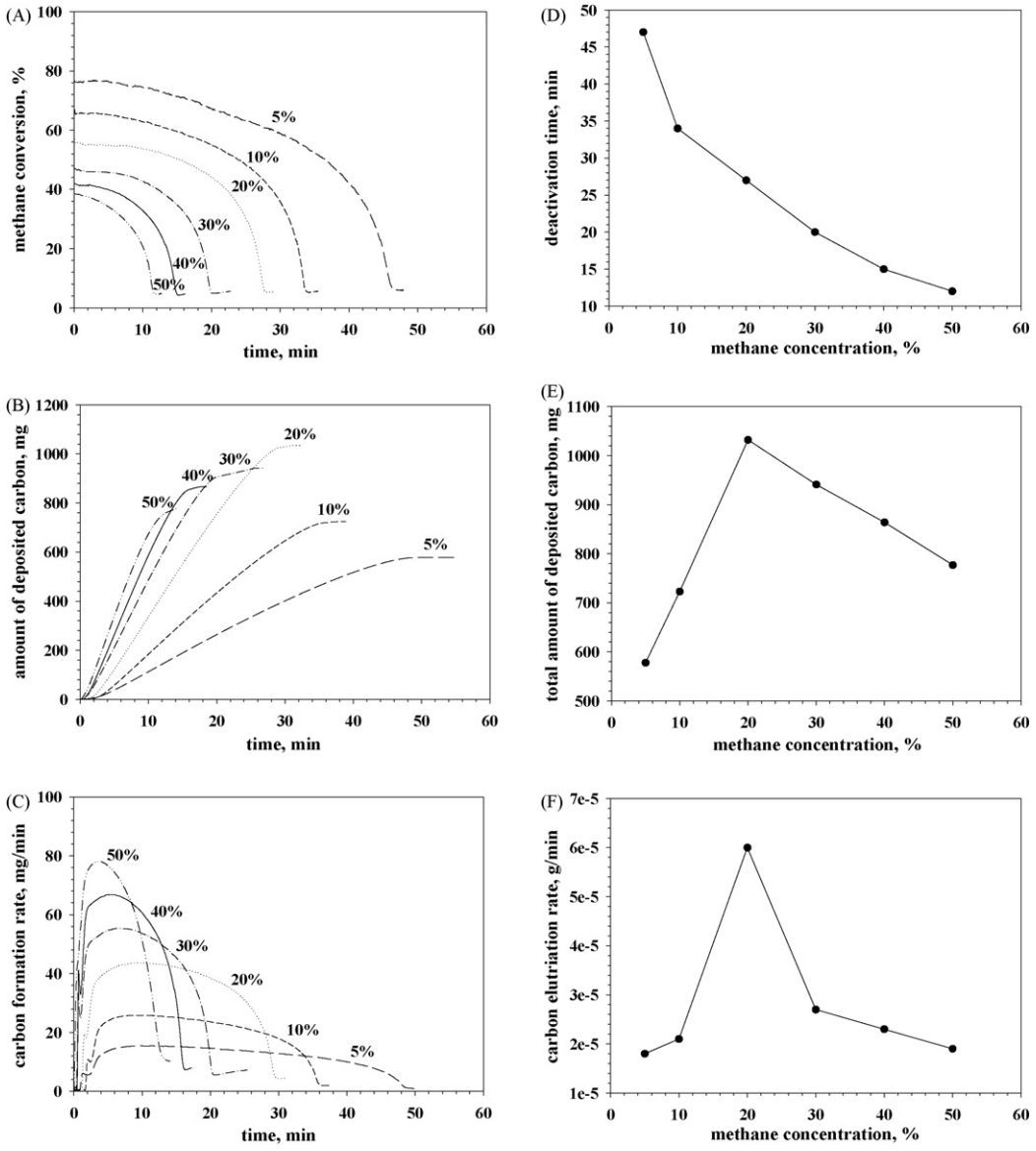

Fig. 5. Effect of methane concentration. Methane conversion (A), amount of deposited carbon (B), carbon formation rate (C), deactivation time (D), total amount of deposited carbon (E), carbon elutriation rate (F). $T = 800\,^{\circ}C$; $m_{cat} = 25\,g$; $Q = 45\,N\,l/h$.

tion rate curves show an initial period of a rapid growth until a maximum is reached. This is followed by a decrease in the carbon formation rate until a residual constant value is reached. The formation rate of carbon increases with methane concentration. Nevertheless, the total carbon amount deposited on the catalyst until deactivation, reported in Fig. 5E, presents a maximum value at 20% of methane concentration. This result highlights that the catalyst deactivation depends not only on the amount but also on the nature of the deposited carbon, depending on the operating conditions. In particular, it is possible the formation of carbon species which can encapsulate and deactivate the active sites depending on the operating conditions [19,20]. The methane concentration has a great effect on the characteristic of carbon deposition: an increase in methane concentration leads to an increase not only in the carbon formation rate but also in the formation of encapsulating carbon species and then in the deactivation rate. Moreover, the catalyst deactivation effect is more marked at higher methane concentrations [20,21]. When the methane concentration is lower than 20% the carbon formation rate is higher than the deactivation rate and vice versa: in consequence, the total carbon amount deposited on the catalyst until deactivation shows a maximum value. This behaviour is different from that observed for Ni-based catalyst, showing an increase in the amount of produced carbon with methane concentration [22]. However, it should be taken into account the different morphology of deposited carbon, since the Ni-based catalysts favour the formation of filamentous carbon. The values of carbon elutriation rate (Fig. 5F), depending on the methane concentration and, then, on the amount of carbon deposited on the catalyst, are relatively low, indicating that under the operating conditions tested, attrition removes only a negligible fraction of the produced carbon from the catalyst surface. This is confirmed by the occurrence of the observed deactivation of the catalyst found during the different experimental tests.

The effect of reaction temperature on methane conversion (A), amount of deposited carbon (B), carbon formation rate (C), deactivation time (D), total amount of carbon deposited on the catalyst (E) and carbon elutriation rate (F) are reported in Fig. 6. The initial methane conversion increases with temperature but a soft decaying is observed at lower temperatures, whereas a rapid fall in methane conversion is observed at higher temperatures. So that the deac-

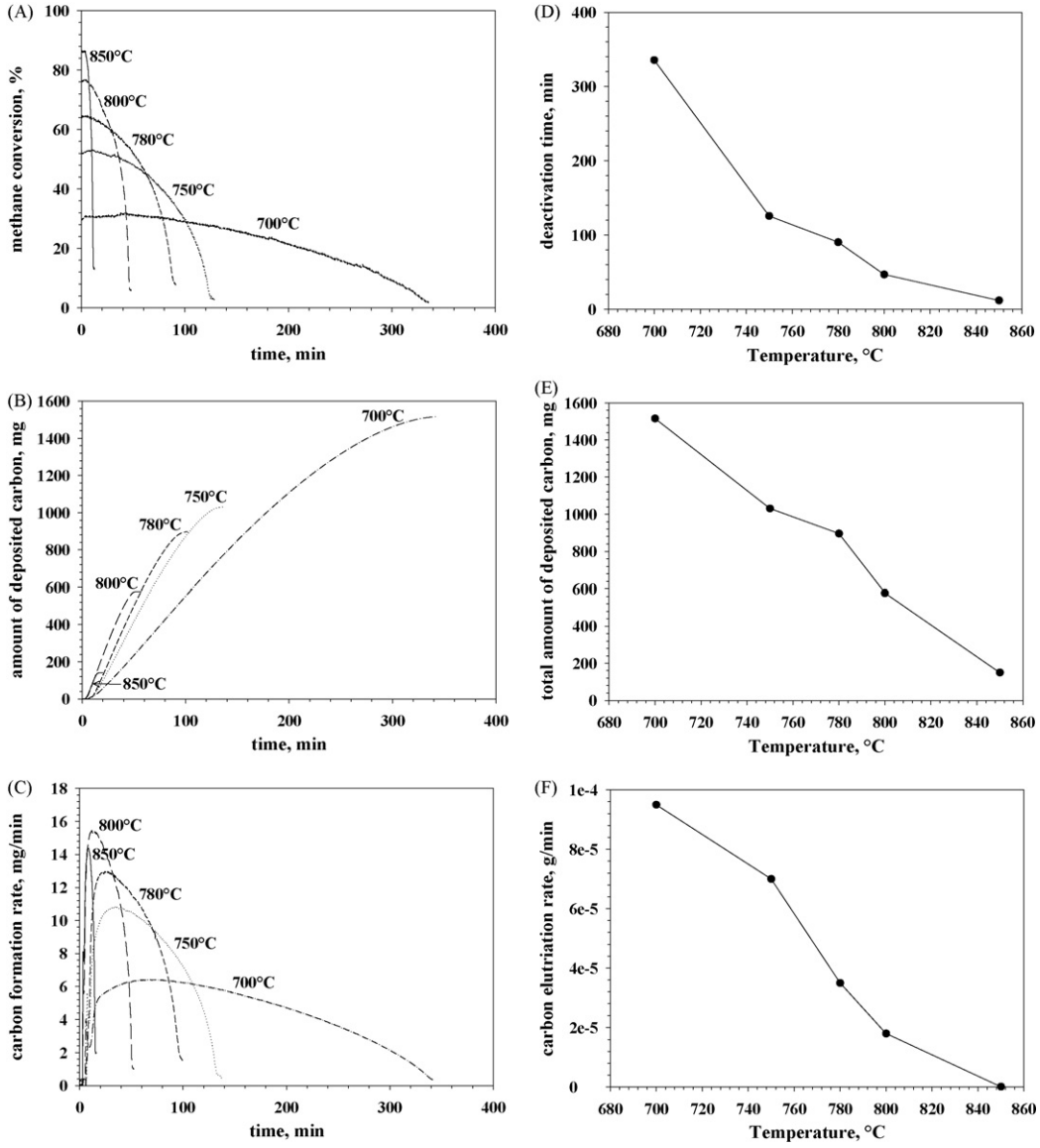

Fig. 6. Effect of reaction temperature. Methane conversion (A), amount of deposited carbon (B), carbon formation rate (C), deactivation time (D), total amount of deposited carbon (E), carbon elutriation rate (F). Feed composition: CH_4 (5 vol.%) in N_2; m_{cat} = 25 g; Q = 45 N l/h.

tivation time decreases with temperature. Also in this case the observed conversions are much lower than the achievable at the equilibrium. This behaviour is expected according to the kinetics controlling regime of the reactor performances. The carbon formation rate increases with temperature. Moreover, the total carbon amount deposited on the catalyst until deactivation significantly decreases with temperature. In particular, only a very small formation of carbon has been observed at the highest temperature

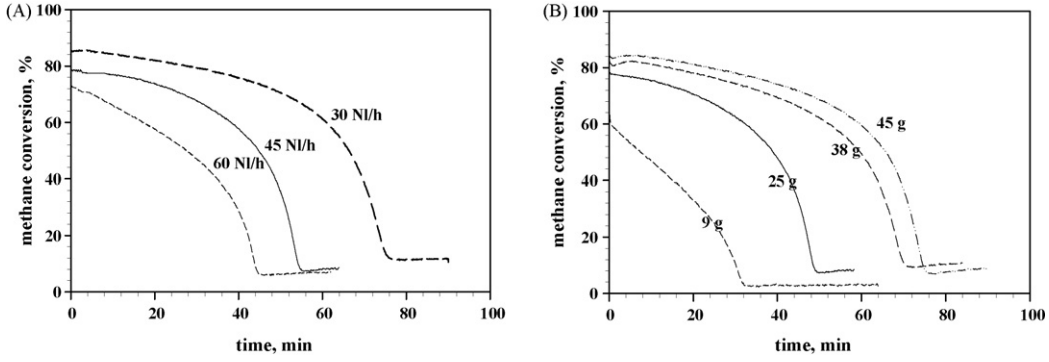

Fig. 7. Methane conversion. (A) Effect of total flow rate. Feed composition: CH_4 (5 vol.%) in N_2; T = 800 °C; m_{cat} = 25 g. (B) Effect of catalyst amount. Feed composition: CH_4 (5 vol.%) in N_2; T = 800 °C; Q = 45 N l/h.

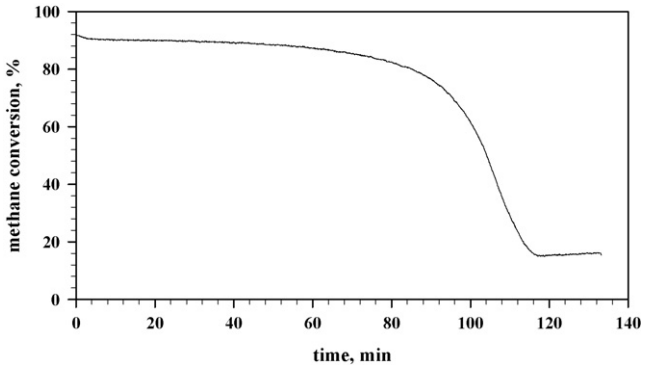

Fig. 8. Methane conversion. Feed composition: CH_4 (5 vol.%) in N_2; T = 800 °C; m_{cat} = 45 g; Q = 30 N l/h.

(850 °C). An increase in the operating temperature favours both the methane decomposition rate and the encapsulating carbon formation. At high temperatures, the catalyst deactivation effect is more marked [20,23]. This explains the reduction in the amount of carbon formed at high temperatures. In comparison with the methane concentration effect, a maximum carbon amount would be expected. Probably, the maximum temperature is lower than 700 °C, the lowest temperature investigated in the present study, according to that reported in literature for Ni-based catalysts [21]. The carbon elutriation rate is generally low under the different conditions.

Methane conversion profiles as function of time obtained for different total gas flow rates and catalyst amounts are reported in Fig. 7A and B, respectively. As expected, both a decrease in the flow rate and an increase in the catalyst amount, i.e. an increase in the gas to particles contact time, involve an increase in both methane conversion and deactivation time. In fact, among the operating conditions tested, in the most favourable case. i.e. at the lowest total flow rate (Q = 30 N l/h) and at the highest catalyst amount (m_{cat} = 45 g), an initial methane conversion degree of about 91%, not very far from the thermodynamic equilibrium value at 800 °C (99.1%), has been kept stable for about 2 h, as reported in Fig. 8. Whatever the operative condition were at fixed methane concentration (5 vol.% in N_2) and reaction temperature (800 °C), the amount of carbon produced per gram of catalyst was always about 24 mg/g_{cat}, i.e. the deposited carbon has always the same nature. This evidence highlights that the methane concentration and the reaction temperature are the only operating conditions controlling the kinetics of methane decomposition and of deactivation and then the nature and the amount of carbon deposited on the catalyst until deactivation. On the other hand, the total flow rate and the catalyst amount do not affect the intrinsic kinetics of methane decomposition, i.e. the controlling step of the process. Relatively low carbon elutriation rates have been obtained. The highest value, 2.7×10^{-5} g/min, has been found operating the bed at the highest flow rate, i.e. the highest superficial gas velocity.

4. Conclusions

The thermo-catalytic decomposition of methane has been investigated in a laboratory scale bubbling fluidized bed reactor, using a copper dispersed on γ-alumina catalyst. The effects of both total flow rate and amount of catalyst, i.e. contact time, as well as of reaction temperature and CH_4 inlet concentration on CH_4 to H_2 conversion, amount of carbon deposited on the catalyst and deactivation time have been investigated. The relevance of attrition phenomena have been also investigated as a useful way to mechanically regenerate the catalyst, removing the carbon deposited on the external surface of catalytic particles.

No pore occlusion of the catalyst particles due to carbon deposition occurs and the carbon produced is uniformly dispersed on the surface of the catalyst, without the formation of filamentous carbon, under the different operating conditions.

Both the decomposition temperature and the methane inlet concentration affect the deactivation time and methane conversion as well as the amount of carbon deposited on the catalyst, due to the relative rates of two competitive phenomena (methane decomposition and catalyst deactivation). Both the total flow rate and catalyst amount affect the deactivation time and methane conversion but they do not affect the amount of deposited carbon/amount of catalyst. In the most favourable case (methane concentration = 5%, reaction temperature = 800 °C, total flow rate = 30 N l/h and catalyst amount = 45 g) a methane conversion of ~90% has been stably obtained for about 90 min. The rate of carbon removal by attrition is relatively low under the experimental conditions tested, indicating that only a negligible fraction of the produced carbon has been removed from the catalyst surface.

The relative importance of interparticle and interphase diffusional processes and of intrinsic kinetics of heterogeneous reaction has been assessed. In all the investigated operating conditions the methane conversion rate is controlled by the intrinsic reaction kinetics, being the mass transfer between bubbles and emulsion phase, the mass transfer in the boundary layer around the catalyst particle and the mass transfer inside the catalyst particle more effective than intrinsic kinetics.

References

[1] N. Muradov, F. Smith, C. Huang, A. T-Raissi, Autothermal catalytic pyrolysis of methane as a new route to hydrogen production with reduced CO_2 emissions, Catal. Today 116 (2006) 281–288.
[2] N. Muradov, T.N. Veziroğlu, From hydrocarbon to hydrogen–carbon to hydrogen economy, Int. J. Hydrogen Energy 30 (2005) 225–237.
[3] N. Muradov, Z. Chen, F. Smith, Fossil hydrogen with reduced CO_2 emission: modeling thermocatalytic decomposition of methane in a fluidized bed of carbon particles, Int. J. Hydrogen Energy 30 (2005) 1149–1158.
[4] K.K. Lee, G.Y. Han, K.J. Yoon, B.K. Lee, Thermocatalytic hydrogen production from the methane in a fluidized bed with activated carbon catalyst, Catal. Today 93–95 (2004) 81–86.
[5] A.M. Dunker, S. Kumar, P.A. Mulawa, Production of hydrogen by thermal decomposition of methane in a fluidized-bed reactor-effects of catalyst, temperature, and residence time, Int. J. Hydrogen Energy 31 (2006) 473–484.
[6] P. Ammendola, G. Ruoppolo, R. Chirone, G. Russo, H_2 production by catalytic methane decomposition in fixed and fluidized bed reactors, in: F. Winter (Ed.), Proceedings of 19th International Conference on Fluidized Bed Combustion, Vienna, Austria, 2006.
[7] N. Shah, S. Ma, Y. Wang, G.P. Huffman, Semi-continuous hydrogen production from catalytic methane decomposition using a fluidized-bed reactor, Int. J. Hydrogen Energy 32 (2007) 3315–3319.
[8] J.L. Pinilla, R. Moliner, I. Suelves, M.J. Lázaro, Y. Echegoyen, J.M. Palacios, Production of hydrogen and carbon nanofibers by thermal decomposition of methane using metal catalysts in a fluidized bed reactor, Int. J. Hydrogen Energy 32 (2007) 4821–4829.
[9] H. Ogihara, S. Takenaka, I. Yamanaka, E. Tanabe, A. Genseki, K. Otsuka, Formation of highly concentrated hydrogen through methane decomposition over Pd-based alloy catalysts, J. Catal. 238 (2006) 353–360.
[10] R. Aiello, J.E. Fiscus, M. Hans-Conrad zur Loye, D. Amiridis, Hydrogen production via the direct cracking of methane over Ni/SiO_2: catalyst deactivation and regeneration, Appl. Catal. A-Gen. 192 (2000) 227–234.
[11] S. Takenaka, S. Kobayashi, H. Ogihara, K. Otsuka, Ni/SiO_2 catalyst effective for methane decomposition into hydrogen and carbon nanofiber, J. Catal. 217 (2003) 79–87.
[12] M.A. Ermakova, D.Y. Ermakov, A.L. Chuvilin, G.G. Kuvshinov, Decomposition of methane over iron catalysts at the range of moderate temperatures: the influence of the catalytic systems and the reaction conditions on the yield of carbon and morphology of carbon filaments, J. Catal. 201 (2001) 183–197.
[13] S. Takenaka, M. Serizawa, K. Otsuka, Formation of filamentous carbons over supported Fe catalysts though methane decomposition, J. Catal. 222 (2004) 520–531.
[14] P. Ammendola, R. Chirone, L. Lisi, G. Ruoppolo, G. Russo, Copper catalysts for H_2 production via CH_4 decomposition, J. Mol. Catal. A-Chem. 266 (2007) 31–39.
[15] D. Geldart, Types of gas fluidization, Powder Technol. 7 (1973) 285–292.
[16] C.Y. Wen, Y.H. Yu, A generalized method for predicting the minimum fluidization velocity, AIChE J. 12 (1966) 610–612.

[17] P. Ammendola, R. Chirone, G. Ruoppolo, G. Russo, R. Solimene, Some issues in modelling methane catalytic decomposition in fluidized bed reactors, Int. J. Hydrogen Energy 33 (2008) 2679–2694.
[18] N. Muradov, CO_2-free production of hydrogen by catalytic pyrolysis of hydrocarbon fuel, Energy Fuel 12 (1998) 41–48.
[19] I. Suelves, M.J. Lázaro, R. Moliner, B.M. Corbella, J.M. Palacios, Hydrogen production by thermo catalytic decomposition of methane on Ni-based catalysts: influence of operating conditions on catalyst deactivation and carbon characteristics, Int. J. Hydrogen Energy 30 (2005) 1555–1567.
[20] J.I. Villacampa, C. Royo, E. Romeo, J.A. Montoya, P. Del Angel, A. Monzón, Catalytic decomposition of methane over Ni–Al_2O_3 coprecipitated catalysts. Reaction and regeneration studies, Appl. Catal. A-Gen. 252 (2003) 363–383.
[21] A. Monzón, N. Latorre, T. Ubieto, C. Royo, E. Romeo, J.I. Villacampa, L. Dussault, J.C. Dupin, C. Guimon, M. Montioux, Improvement of activity and stability of Ni–Mg–Al catalysts by Cu addition during hydrogen production by catalytic decomposition of methane, Catal. Today 116 (2006) 264–270.
[22] L. Piao, Y. Li, J. Chen, L. Chang, J.Y.S. Lin, Methane decomposition to carbon nanotubes and hydrogen on an alumina supported nickel aerogel catalyst, Catal. Today 74 (2002) 145–155.
[23] V.R. Choudhary, S. Banerjee, A.M. Rajput, Hydrogen from step-wise steam reforming of methane over Ni/ZrO_2: factors affecting catalytic methane decomposition and gasification by steam of carbon formed on the catalyst, Appl. Catal. A-Gen. 234 (2002) 259–270.